JOURNAL OF COMPUTATIONAL PHYSICS **141,** 153–173 (1998)
ARTICLE NO. CP985914

A Unified Method for Computing Incompressible and Compressible Flows in Boundary-Fitted Coordinates

Hester Bijl[1] and Pieter Wesseling

J. M. Burgers Center and TU Delft, Mekelweg 4, 2628 CD Delft, The Netherlands
E-mail: h.bijl@math.tudelft.nl

Received July 7, 1997; revised December 15, 1997

A unified method for computing incompressible and compressible flows with Mach-uniform accuracy and efficiency is described. The method is equally applicable to stationary and nonstationary flows. A pressure-based discretisation on a staggered grid in general boundary-fitted coordinates is used for the Euler equations. Extension to Navier–Stokes is straightforward. Dimensionless variables that remain finite for all Mach numbers are used. Mach number independent accuracy and efficiency is shown by numerical experiments.

Key Words: finite volume method; boundary-fitted coordinates; Euler equations compressible flow; subsonic flow; transonic flow; supersonic flow.

1. INTRODUCTION

When the Mach number in a flow is uniformly low, say below 0.2, solution can take place with equations and numerical methods assuming incompressibility. When the Mach number is higher, the compressible flow equations need to be employed, and numerical methods different from those for the incompressible case are used. This leaves us with the question: what to do when both low and high Mach numbers occur simultaneously in a flow?

What is needed is a method with Mach-uniform accuracy and efficiency, both as the Mach number $M \downarrow 0$ and when $M = \mathcal{O}(1)$. Straightforward use of standard compressible methods gives severe convergence problems or even breakdown in the presence of regions with very low Mach number. Therefore efforts have been made to develop special methods for such flows.

[1] Supported by the Dutch Technology Foundation (STW).

0021-9991/98 $25.00

For low speed variable density flows asymptotic methods based on series expansion in the Mach number have been developed in [9, 23, 30]. Such methods can only be used when the Mach number is small enough (less than 0.3 say). Another approach is to improve the low Mach number behavior of compressible methods. Because large investments have been made in codes for compressible flows, much work has been done in this direction. Extension to low Mach numbers can be done by preconditioning [2, 4, 8, 36, 43, 44, 47, 49]. Another possibility is to perturb the equations with artificial compressibility, replacing the physical acoustic modes by artificial acoustic modes [3, 9, 15, 27–29, 33, 48, 51]. These measures usually falsify the time dependence, making time-accurate unsteady computations awkward or inefficient. Also, usually very small Mach numbers (less than 0.05, say) cannot be handled, or only at increasing expense, and the limit $M \downarrow 0$ is frequently singular. Such low Mach numbers are encountered in flows with combustion or in stratified atmospheric flows. Another type of method is proposed by Patnaik *et al.* [32]; here the density is stepped forward in time by the continuity equation, and a pressure correction is derived from the energy equation. The method can compute sound waves and nonstationary weakly compressible flows. It would seem that this method does not reduce to a well-known incompressible method as $M \downarrow 0$. All of the above methods use nonstaggered grids.

Alternatively, one may extend an incompressible method to the compressible case. Obviously, this gives the best prospects for handling the limit $M \downarrow 0$, assuming that in this limit a well-proven incompressible scheme is recovered. With a nonstaggered scheme this has been done by Demirdžić *et al.* [6]. A staggered grid was first used to compute compressible flows by Harlow and Amsden [10, 11], generalizing the MAC scheme of Harlow and Welch [12] to the compressible case, in orthogonal coordinates. Later works in this direction, using general coordinates, are [17, 18, 20, 36, 38, 39]. This is also the approach taken by us here. Staggered schemes have not caught on for compressible flows, because they seem to offer no advantage over nonstaggered schemes and are more complicated to implement accurately in general coordinates. However, for incompressible flows they are attractive, because no artificial measures need to be taken to avoid spurious pressure oscillations and the physical boundary conditions suffice. Furthermore, for the incompressible case recently accurate staggered discretizations in general coordinates have appeared; some references, apart from those just quoted, are [5, 16, 24, 34, 42, 52, 53]. Given an accurate staggered scheme in general coordinates, inclusion of compressibility is quite feasible along the lines already laid out by Harlow and Amsden. Inclusion of accurate and efficient time discretization is in fact easier than for nonstaggered schemes, because there are no artificial regularizing terms. Furthermore, as some of the test cases to be described show, accuracy and efficiency of a staggered scheme turn out to compare quite well with standard schemes in the fully compressible case.

Here we will generalize the incompressible staggered scheme in general coordinates described by Zijlema *et al.* [52, 53] to the nonstationary compressible case. We specialize to the Euler equations, because with our approach viscosity plays no role in the difficulties associated with $M \downarrow 0$. Generalization to Navier–Stokes is straightforward. This will, therefore, not be explained, and we will only show results obtained for the Navier–Stokes equations. Compared to the earlier work quoted above, we unify the following two existing methodologies, combining their advantages:

(a) a nondimensionalization similar to that of Shuen *et al.* [36] that eliminates the singularity associated with $M \downarrow 0$;

(b) a general coordinate version of the staggered grid method of Harlow and Amsden [10, 11], similar to that of Shyy [38, 39].

Shuen *et al.* [36] use a colocated scheme for compressible flows extended to weakly compressible flows by preconditioning, falsifying transients, and not allowing using $M = 0$. Shyy [38, 39] does not eliminate the singularity associated with $M \downarrow 0$, which we do by our special nondimensionalization. This avoids a difficulty hinted at on page 203 of Harlow and Amsden [11], where it is advised to work with a scaled variable in solving the pressure equation under certain circumstances, and the stabilizing mass diffusion term used in [11] is not needed here.

We can prescribe the Mach number to be arbitrarily small, including zero, in which case the incompressible scheme of Harlow and Welch [12] (in orthogonal coordinates) or that of Zijlema *et al.* [52, 53] (in general coordinates) is recovered. Moreover, temporal accuracy is obtained in a simple manner, without introducing a pseudo-time variable and dual time stepping, as required in many of the works quoted above. Finally, we demonstrate surprisingly good performance of the scheme in the fully compressible case.

For stationary problems, time-stepping to steady state is less efficient than applying a well-designed iterative method to the stationary discretised equations, but we use time-stepping here to show the feasibility of the method to obtain time-accurate solutions, which are harder to compute than stationary solutions in the presence of low Mach number effects.

In Section 2 the dimensionless Euler equations and boundary conditions are presented. The discretisation and solution method are described in Section 3. Section 4 gives numerical results, showing Mach-uniform accuracy and efficiency.

2. DIMENSIONLESS EQUATIONS

The Euler equations are considered. Pressure is used as the primitive variable instead of density, in order to handle the limit $M \downarrow 0$. For brevity the equations are presented in Cartesian tensor notation, although in fact they are solved in general coordinates. The dimensional governing equations are

$$\left(\frac{\partial \rho}{\partial p}\right)_h \frac{\partial p}{\partial t} + \left(\frac{\partial \rho}{\partial h}\right)_p \frac{\partial h}{\partial t} + (\rho u^\alpha)_{,\alpha} = 0, \tag{1}$$

$$\frac{\partial \rho u^\alpha}{\partial t} + (\rho u^\alpha u^\beta)_{,\beta} = -p_{,\alpha}, \tag{2}$$

$$\frac{\partial h}{\partial t} + u^\alpha h_{,\alpha} = -(\gamma - 1) h u^\alpha_{,\alpha}, \tag{3}$$

where $u^\alpha = u_\alpha$ are the Cartesian velocity components, ρ is the density, p is the pressure, h is the enthalpy, and γ is the specific heat ratio. The equation of state for an ideal gas completes the system of equations:

$$\rho = \frac{\gamma}{\gamma - 1} \frac{p}{h}. \tag{4}$$

Although a nonconservative form for the energy equation is used, the numerical scheme to be used turns out to converge to genuine weak solutions. The above nonconservative form is merely used for greater efficiency in the pressure correction time stepping scheme to be described and could be replaced by the conservative form.

We will discuss internal flow in a two-dimensional channel or nozzle. The inflow and outflow boundaries are referred to by subscripts $_\infty$ and $_{out}$, respectively. When the inflow is subsonic, h_∞, p_{out}, and u^α_∞, $\alpha = 1, 2$, are given. For supersonic inflow, all variables should be specified on the inlet boundary, so instead of the pressure at the outflow boundary, p_∞ is given at the inflow boundary. On solid boundaries the impermeability condition is prescribed: $u_\alpha n^\alpha = 0$ with $\mathbf{n}$ the normal on the solid wall. The initial conditions specify p, u^α, and h.

The equations are made dimensionless by scaling the variables by reference quantities ρ_r, h_r, p_r, w_r, the reference speed, and L_r, the reference length, that still remain to be chosen. The time is nondimensionalised by L_r/w_r. The following dimensionless Euler equations are obtained:

$$\frac{\partial \rho}{\partial t} + (\rho u^\alpha)_{,\alpha} = 0, \tag{5}$$

$$\frac{\partial \rho u^\alpha}{\partial t} + (\rho u^\alpha u^\beta)_{,\beta} + \frac{p_r}{\rho_r w_r^2} p_{,\alpha} = 0, \tag{6}$$

$$\frac{\partial h}{\partial t} + u^\alpha h_{,\alpha} = -(\gamma - 1) h u^\alpha_{,\alpha}. \tag{7}$$

In the standard compressible formulation the density is used as the primitive variable, and the pressure follows from the equation of state, so, quite naturally, for p_r the following choice is usually made:

$$p_r = \rho_r R T_r. \tag{8}$$

Hence the factor $p_r/\rho_r w_r^2$ in the dimensionless momentum equation (6) becomes

$$\frac{p_r}{\rho_r w_r^2} = \frac{\rho_r R T_r}{\rho_r w_r^2} = \frac{a_r^2}{\gamma w_r^2} = \frac{1}{\gamma M_r^2}. \tag{9}$$

Therefore in the incompressible limit $M_r \downarrow 0$ the momentum equations (6) degenerate to $p_{,\alpha} = 0$. Detailed mathematical analysis [21, 22, 25, 26] reveals that limit $M_r \downarrow 0$ of the compressible Euler and Navier–Stokes equations is singular. In this limit the solution of the compressible equations does not converge to the solution of the incompressible equations, but to the incompressible solution plus an acoustic field. The acoustic field disappears when the initial conditions are chosen in a special way.

In order to obtain a Mach-uniform formulation in which the limit $M \downarrow 0$ is regular the pressure is made dimensionless in a different way. In Panton [31] it is shown that the dimensionless pressure gradient is of the same order as the inertia terms if p_r is equal to $\rho_r w_r^2$, that is, if the dimensionless pressure is defined to be

$$p = \frac{p^* - p_c^*}{\rho_r w_r^2},$$

with p_c^* a constant pressure level still to be chosen. A similar dimensionless pressure is introduced by Shuen *et al.* [36]. This results in the following dimensionless form of the Euler equations:

$$\left(\frac{\partial \rho}{\partial p}\right)_h \frac{\partial p}{\partial t} + \left(\frac{\partial \rho}{\partial h}\right)_p \frac{\partial h}{\partial t} + (\rho u)^\alpha_{,\alpha} = 0, \tag{10}$$

$$\frac{\partial(\rho u)^\alpha}{\partial t} + ((\rho u)^\alpha u^\beta)_{,\beta} = -p_{,\alpha}, \tag{11}$$

$$\frac{\partial h}{\partial t} + u^\alpha h_{,\alpha} = -(\gamma - 1) h u^\alpha_{,\alpha}. \tag{12}$$

Reference values based on boundary conditions and reservoir parameters are used. The resulting formulation is different from that used by Shyy *et al.* [38–40]. The Mach number at the inlet is defined by

$$M_\infty = \frac{w^*_\infty}{a^*_\infty}, \tag{13}$$

where w^*_∞ is the velocity of the flow and $a^*_\infty = \sqrt{(\gamma - 1)h^*_\infty}$ is the speed of sound. The reference quantities are chosen equal to the stagnation condition at the inlet, denoted by subscript 0:

$$h^*_0 = \left(1 + \frac{\gamma - 1}{2} M^2_\infty\right) h^*_\infty, \tag{14}$$

$$a^{*2}_0 = \left(1 + \frac{\gamma - 1}{2} M^2_\infty\right) a^{*2}_\infty, \tag{15}$$

$$\rho^*_0 = \left(1 + \frac{\gamma - 1}{2} M^2_\infty\right)^{1/(\gamma-1)} \rho^*_\infty, \tag{16}$$

$$p^*_0 = \left(1 + \frac{\gamma - 1}{2} M^2_\infty\right)^{\gamma/(\gamma-1)} p^*_\infty. \tag{17}$$

The dimensionless variables are defined by

$$x^\alpha = \frac{x^{\alpha *}}{L^*}, \qquad t = \frac{t^* w^*_\infty}{L^*},$$

$$p = \frac{p^* - p^*_{out}}{\rho^*_0 w^{*2}_\infty}, \qquad h = \frac{h^*}{h^*_0},$$

$$\rho = \frac{\rho^*}{\rho^*_0}, \qquad u^\alpha = \frac{u^{\alpha *}}{w^*_\infty}, \qquad \alpha = 1, 2,$$

where we have chosen $p^*_c = p^*_{out}$. The equation of state (4) becomes

$$\rho = \rho(p, h) = \frac{\gamma M^2_\infty}{1 + \frac{\gamma-1}{2} M^2_\infty} \frac{p}{h} + \left[p_v \left(\left(1 + \frac{\gamma - 1}{2} M^2_\infty\right)^{-\gamma/(\gamma-1)} - 1 \right) + 1 \right] \frac{1}{h}, \tag{18}$$

where p_v is defined by

$$p_v = \frac{p^*_{out} - p^*_0}{p^*_\infty - p^*_0}. \tag{19}$$

The dimensionless equation of state shows that ρ becomes independent of p as $M_\infty \downarrow 0$, which is precisely what we want, because this eliminates acoustic modes. Furthermore,

in this limit the variation of p remains $\mathcal{O}(1)$. This dimensionless formulation includes the incompressible case, which is obtained by putting $M_\infty = 0$.

The dimensionless subsonic boundary conditions become

$$\begin{aligned}
(\rho u)^1_\infty &= \left(1 + \frac{\gamma-1}{2} M^2_\infty\right)^{-1/(\gamma-1)} \cos\alpha_\infty, \\
(\rho u)^2_\infty &= \left(1 + \frac{\gamma-1}{2} M^2_\infty\right)^{-1/(\gamma-1)} \sin\alpha_\infty, \\
h_\infty &= \left(1 + \frac{\gamma-1}{2} M^2_\infty\right)^{-1}, \\
p_{out} &= 0.
\end{aligned} \tag{20}$$

For the supersonic inflow p_∞ must be prescribed instead of p_{out}.

3. DISCRETISATION AND PRESSURE CORRECTION METHOD

3.1. *Invariant Formulation*

For computing flows in general domains the governing equations are written in coordinate-invariant form, using tensor notation,

$$\left(\frac{\partial \rho}{\partial p}\right)_h \frac{\partial p}{\partial t} + \left(\frac{\partial \rho}{\partial h}\right)_p \frac{\partial h}{\partial t} + (\rho U)^\alpha_{,\alpha} = 0, \tag{21}$$

$$\frac{\partial (\rho U)^\alpha}{\partial t} + ((\rho U)^\alpha U^\beta)_{,\beta} = -(g^{\alpha\beta} p)_{,\beta}, \tag{22}$$

$$\frac{\partial h}{\partial t} + U^\alpha h_{,\alpha} = -(\gamma - 1) h U^\alpha_{,\alpha}, \tag{23}$$

with $(\rho U)^\alpha = \mathbf{a}^{(\alpha)} \cdot (\rho \mathbf{u})$ the contravariant momentum components and where the contravariant metric tensor and base vectors are defined as

$$g^{\alpha\beta} = \mathbf{a}^{(\alpha)} \cdot \mathbf{a}^{(\beta)}, \quad \mathbf{a}^{(\alpha)} = \frac{\partial \xi^\alpha}{\partial \mathbf{x}}. \tag{24}$$

Here, $\mathbf{x}$ are Cartesian coordinates in the physical domain Ω, and ξ are boundary-conforming curvilinear coordinates corresponding to Cartesian coordinates in the computational domain G. For more details see [52, 53].

3.2. *Discretisation in Space in General Coordinates*

The compressible Euler equations will be discretised in space in boundary-fitted coordinates using a finite volume scheme on a staggered grid for the reasons given in Section 1. The scheme is designed such that as $M_\infty \downarrow 0$ the classical incompressible staggered grid method of Harlow and Welch [12] is recovered (in the Cartesian case). This may be expected to give Mach-independent accuracy and efficiency for small and medium Mach numbers. Figure 1 shows part of the computational grid with the staggered placement of the unknowns and the corresponding control volumes. The discretisation in general coordinates introduces mass

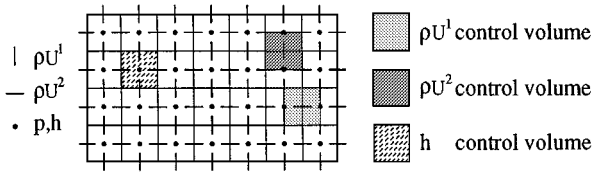

FIG. 1. Grid in computational domain G.

flux components ρV^α, $V^\alpha = \sqrt{g}U^\alpha$, $g = \det(g^{\alpha\beta})$. The invariant discretisation in general coordinates of the incompressible Navier–Stokes equations is described in [35, 52, 53].

In subsonic flow second-order central discretisation is used for the spatial derivatives, and the goal of Mach-uniform accuracy and efficiency is achieved, as will be seen. In the case of transonic flows this scheme did not converge. Some form of irreversibility needs to be built in to satisfy the entropy condition. Therefore, a first-order upwind scheme was used for the energy equation. This proved to be sufficient for transonic flows, whereas for supersonic flows upwind discretisation for the momentum equations appeared to be necessary as well. The simple first-order upwind scheme is used to show that the scheme is also quite satisfactory for fully compressible flow. In order to obtain second-order accurate results and crisp resolution of contact discontinuities the same measures can be taken as for standard compressible methods, such as implementation of higher order upwind biased TVD schemes with flux limiting. In this way the higher order MUSCL scheme was implemented (see Section 4.3). The present scheme compares well with the first-order Godunov scheme for fully compressible flows, as will be seen.

In supersonic regions the density is biased in the upstream direction in the continuity equation, in order to satisfy the entropy condition. This was done using a Mach-dependent shift operator. Assuming U^1 to be the dominant velocity component, this is done as follows. In cells with a Mach number lower than $1 - d$, with d a parameter to be chosen (in the following, $d = 0.1$), no upstream bias is employed and central interpolation is used to evaluate the density in the velocity points. For cells with a Mach number above $1 - d$ the density in the continuity equation is shifted upstream using

$$\left(\frac{\partial\rho}{\partial p}\right)_h \frac{\partial p}{\partial t} + \left(\frac{\partial\rho}{\partial h}\right)_p \frac{\partial h}{\partial t} + \left(\frac{\tilde{\rho}}{\rho}(\rho V)^1\right)\Bigg|_{i-1/2,j}^{i+1/2,j} + (\rho V)^2\Big|_{i,j-1/2}^{i,j+1/2} = 0, \tag{25}$$

with $\rho_{i+1/2,j} = \frac{1}{2}(\rho_{i,j} + \rho_{i+1,j})$ as the centrally evaluated density and $\tilde{\rho}_{i+1/2,j}$ as the shifted evaluation of the density, given by

$$\tilde{\rho}_{i+1/2,j} = (0.5 - S_{i+1/2,j})\rho_{i+1,j} + (0.5 + S_{i+1/2,j})\rho_{i,j}. \tag{26}$$

Here S is a continuous switch function defined by

$$S_{i+1/2,j} = S\big(V^1_{i+1/2,j}, M_{i+1/2,j}\big) = \frac{V^1_{i+1/2,j}}{\big|V^1_{i+1/2,j}\big|} \min\left(\frac{1}{2}, \max\left(0, \frac{1}{4}\left(\frac{M_{i+1/2,j} - 1}{d} + 1\right)\right)\right). \tag{27}$$

The local Mach number in the cell center is computed as:

$$M^2_{i,j} = \frac{M^2_\infty}{1 + \frac{\gamma-1}{2}M^2_\infty} \frac{\big(V^1_{i+1/2,j} + V^1_{i-1/2,j}\big)^2 + \big(V^2_{i,j+1/2} + V^2_{i,j-1/2}\big)^2}{4g\rho^2_{i,j}h_{i,j}}. \tag{28}$$

$M_{i+1/2,j}$ is found through linear interpolation. The switch function S varies between 0 (no bias) for $M < 1-d$ to $\frac{1}{2}$ (full bias) for $M > 1+d$.

3.3. *Pressure Correction Method*

In the incompressible case there is no time-derivative for the pressure. This is also the case in the present Mach-uniform formulation, as it should be; for $M = 0$ the factor $\partial\rho/\partial p$ in Eq. (25) is zero, according to the dimensionless equation of state. The standard workhorse to do time-stepping in the incompressible case is the pressure correction method, already introduced by Harlow and Welch [12]. This method will also be employed here, for all Mach numbers, in order to achieve Mach-uniform accuracy and efficiency.

For brevity, we leave the spatial derivatives undiscretised and write m^α for ρU^α. In practice we discretise in space and incorporate the boundary conditions before discretising in time. The continuity and momentum equations are discretised in time as follows:

$$\left(\frac{\partial\rho}{\partial p}\right)_h^n \frac{p^{n+1}-p^n}{\delta t} + \left(\frac{\partial\rho}{\partial h}\right)_p^n \frac{h^{n+1}-h^n}{\delta t} + \mu\left(m^\alpha_{,\alpha}\right)^{n+1} + (1-\mu)\left(m^\alpha_{,\alpha}\right)^n = 0, \quad (29)$$

$$\frac{(m^\alpha)^{n+1}-(m^\alpha)^n}{\delta t} + \theta((m^\alpha)^{n+1}(U^\beta)^n)_{,\beta} + (1-\theta)(m^\alpha U^\beta)^n_{,\beta} = -(g^{\alpha\beta}(\mu p^{n+1} + (1-\mu)p^n))_{,\beta}. \quad (30)$$

Depending on the parameters μ and θ, the discretisation is explicit or implicit. But in the incompressible case it is needed to take $\mu = 1$, because then the pressure acts as a Lagrangian multiplier to satisfy the divergence freedom constraint. With the pressure correction method, first, a prediction for the momentum field $m^{\alpha *}$ is computed from

$$\frac{(m^\alpha)^*-(m^\alpha)^n}{\delta t} + \theta((m^\alpha)^*(U^\beta)^n)_{,\beta}(1-\theta)(m^\alpha U^\beta)^n_{,\beta} = -(g^{\alpha\beta}p^n)_{,\beta}. \quad (31)$$

Next, a pressure correction $\delta p = p^{n+1} - p^n$ is computed. To find the correction equation, first (31) is subtracted from (30), neglecting the difference in the convection terms:

$$\frac{(m^\alpha)^{n+1}-(m^\alpha)^*}{\delta t} = -\mu(g^{\alpha\beta}(p^{n+1}-p^n))_{,\beta}. \quad (32)$$

Van Kan [45] has shown for the incompressible case that neglecting the difference in the convection term does not deteriorate the temporal accuracy, and $\theta = 1/2$, $\mu = 1$ gives second-order accuracy in time. Here, in the compressible case, at least first-order accuracy is maintained. Next, the discrete divergence of the discretised version of (32) is taken, and the resulting expression for $(m^\alpha_{,\alpha})^{n+1}$ is substituted in (29), which results in

$$\left(\frac{\partial\rho}{\partial p}\right)_h^n \frac{\delta p}{\delta t} - \mu^2\delta t(g^{\alpha\beta}\delta p)_{,\alpha\beta} = -\mu(m^\alpha)^*_{,\alpha} + (1-\mu)(m^\alpha)^n_{,\alpha} - \left(\frac{\partial\rho}{\partial h}\right)_p^n \frac{\delta h}{\delta t}. \quad (33)$$

This is called the pressure correction equation. For the computation of $\partial\rho/\partial p$ and $\partial\rho/\partial h$ the nondimensional equation of state (18) is used. When $\delta h = h^{n+1} - h^n$ is known, the pressure correction δp can be computed from (33), whereafter $(m^\alpha)^{n+1}$ can be found from

(32). The δh can be computed from the following discretisation of the energy equation:

$$\frac{h^{n+1}-h^n}{\delta t}+(U^\alpha)^n\left(\theta h^{n+1}_{,\alpha}+(1-\theta)h^n_{,\alpha}\right)=-(\gamma-1)(U^\alpha)^n_{,\alpha}(\theta h^{n+1}+(1-\theta)h^n). \quad (34)$$

To obtain at the end of a time step the velocity components $(U^\alpha)^{n+1}$ from $(m^\alpha)^{n+1}$, the mass fluxes are divided by ρ^{n+1}, which is computed from the equation of state. In practice the Euler equations are first discretised in space before the pressure correction method is applied, so that the equations derived in this section are linear algebraic systems. No boundary conditions for the pressure correction equation are required, since the physical velocity and pressure boundary conditions have already been incorporated in the continuity and momentum equations, from which the pressure correction equation is derived. The spatial discretisation in general coordinates is described in [52, 53].

It is instructive to write down the fully discrete scheme for the one-dimensional case. We write $\lambda=\delta t/\delta x$, $m^1=m$, $\delta p=p^{n+1}-p^n$, etc. The discrete continuity equation with density bias is given by, writing $\sigma=\tilde{\rho}/\rho$ (see (26)),

$$\delta\rho_j+\mu\lambda(\sigma m)^{n+1}\big|^{j+1/2}_{j-1/2}+(1-\mu)\lambda(\sigma m)^n\big|^{j+1/2}_{j-1/2}=0. \quad (35)$$

This equation is Newton-linearised as

$$(\sigma m)^{n+1}\approx\sigma^n m^{n+1}+u^n\delta\tilde{\rho}-(u\sigma)^n\delta\rho. \quad (36)$$

This results in the discrete continuity equation

$$\delta\rho_j+\mu\lambda(\sigma^n m^{n+1}+u^n\delta\tilde{\rho}-u^n\sigma^n\delta\rho)\big|^{j+1/2}_{j-1/2}+(1-\mu)\lambda(\sigma m)^n\big|^{j+1/2}_{j-1/2}=0. \quad (37)$$

It is assumed that $u>0$ and that the flow is supersonic, so that the first-order upwind scheme is used and the density bias is in full force. This means that the switch function S in (27) is equal to $\frac{1}{2}$, so that $\delta\tilde{\rho}_{j+1/2}=\delta\rho_j$. As a result the continuity equation (37) becomes

$$\begin{aligned}&\delta\rho_j+\mu\lambda\left(\sigma^n_{j+1/2}m^{n+1}_{j+1/2}+u^n_{j+1/2}\delta\rho_j-u^n_{j+1/2}\sigma^n_{j+1/2}\frac{1}{2}(\delta\rho_{j+1}+\delta\rho_j)\right)\\&-\mu\lambda\left(\sigma^n_{j-1/2}m^{n+1}_{j-1/2}+u^n_{j-1/2}\delta\rho_{j-1}-u^n_{j-1/2}\sigma^n_{j-1/2}\frac{1}{2}(\delta\rho_j+\delta\rho_{j-1})\right)\\&+(1-\mu)\lambda\left(\sigma^n_{j+1/2}m^n_{j+1/2}-\sigma^n_{j-1/2}m^n_{j-1/2}\right)=0. \quad (38)\end{aligned}$$

In this equation $\delta\rho_j$ will be replaced by $(\partial\rho/\partial p)^n_j\delta p_j+(\partial\rho/\partial h)^n_j\delta h_j$. In the solution procedure, first, δh is computed from

$$\begin{aligned}&h^{n+1}_j-h^n_j+\frac{1}{2}\theta\lambda\left(u^n_{j-1/2}+u^n_{j+1/2}\right)h^{n+1}\Big|^j_{j-1}+\frac{1}{2}(1-\theta)\lambda\left(u^n_{j-1/2}+u^n_{j+1/2}\right)h^n\Big|^j_{j-1}\\&+\theta\lambda(\gamma-1)h^{n+1}_j u^n\Big|^{j+1/2}_{j-1/2}+(1-\theta)\lambda(\gamma-1)h^n_j u^n\Big|^{j+1/2}_{j-1/2}=0. \quad (39)\end{aligned}$$

Next, the momentum is predicted according to

$$m^*_{j+1/2}-m^n_{j+1/2}+\theta\lambda(u^n m^*)\big|^{j+1/2}_{j-1/2}+(1-\theta)\lambda(u^n m^n)\big|^{j+1/2}_{j-1/2}+\lambda p^n\big|^{j+1}_j=0. \quad (40)$$

The momentum correction is defined by

$$m_{j+1/2}^{n+1} - m_{j+1/2}^{*} = -\mu\lambda\, \delta p\big|_{j}^{j+1}. \tag{41}$$

When this equation for $m_{j+1/2}^{n+1}$ and $m_{j-1/2}^{n+1}$ is substituted into the continuity equation (38) divided by $\mu\lambda$, the pressure correction equation is found to be

$$-a_{j-1}\delta p_{j-1} + b_j \delta p_j - c_{j+1}\delta p_{j+1} = f_j, \tag{42}$$

where

$$a_{j-1} = (\mu\lambda)\sigma_{j-1/2}^{n} + \left(\frac{\partial\rho}{\partial p}\right)_{j-1}^{n}\left(u_{j-1/2}^{n} - \frac{1}{2}(\sigma u)_{j-1/2}^{n}\right), \tag{43}$$

$$b_j = (\mu\lambda)\left(\sigma_{j+1/2}^{n} + \sigma_{j-1/2}^{n}\right) + \left(\frac{\partial\rho}{\partial p}\right)_{j}^{n}\left\{\frac{1}{\mu\lambda} + u_{j+1/2}^{n} - \frac{1}{2}(\sigma u)_{j+1/2}^{n} - (\sigma u)_{j-1/2}^{n}\right\}, \tag{44}$$

$$c_{j+1} = (\mu\lambda)\sigma_{j+1/2}^{n} + \frac{1}{2}\left(\frac{\partial\rho}{\partial p}\right)_{j+1}^{n}(\sigma u)_{j+1/2}^{n}, \tag{45}$$

$$\begin{aligned} f_j = &-\left(\sigma^n m^* + \left(\frac{1}{\mu} - 1\right)\sigma^n m^n\right)\Big|_{j-1/2}^{j+1/2} - \delta h_{j-1}\left(\frac{\partial\rho}{\partial h}\right)_{j-1}^{n}\left(u_{j-1/2}^{n} - \frac{1}{2}(\sigma u)_{j-1/2}^{n}\right) \\ &- \delta h_j\left(\frac{\partial\rho}{\partial h}\right)_{j}^{n}\left\{\frac{1}{\mu\lambda} + \left(u_{j+1/2}^{n} - \frac{1}{2}(\sigma u)_{j-1/2}^{n}\right|^{j+1/2}\right)\right\} \\ &- \delta h_{j+1}\left(\frac{\partial\rho}{\partial h}\right)_{j+1}^{n}\left(-\frac{1}{2}(\sigma u)_{j+1/2}^{n}\right). \end{aligned} \tag{46}$$

Our main goal here is to show Mach-uniform efficiency and accuracy. For computation of both the steady states of stationary flows and time-accurate solutions of nonstationary problems time-stepping was used. This method is for stationary problems less efficient than applying a well-designed iterative method to the stationary discretised equations. It suffices to show that the given solver does not degrade as $M \downarrow 0$ or when the flow becomes supersonic. In the subsonic case, the spatial discretisation is fully central and the time step must be small enough to sufficiently enhance the main diagonals of the systems for the mass flux components and enthalpy, if an implicit scheme is used. There is a trade-off here between size of time-step and number of iterations per time-step. All systems were solved by a Krylov subspace iterative method for unsymmetric matrices, namely GMRES (see Vuik [50]). This method was preconditioned by ILU. Note that only systems for one variable at a time need to be solved, which makes optimizing iterative solvers much easier than when coupled systems are involved. The pressure correction equation is always weakly diagonally dominant.

4. NUMERICAL RESULTS

4.1. *Introduction*

Two stationary test problems especially suited for testing computating methods with varying Mach numbers have been selected. The first is flow through a channel with a bump,

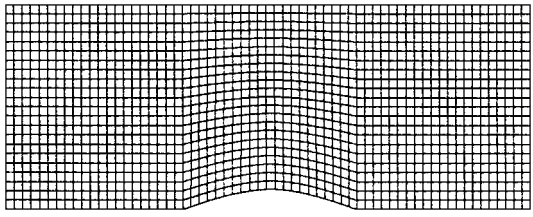

FIG. 2. Grid size 63×22 used for subsonic and transonic computations.

also treated in [7, 19, 20, 38]. The second is flow through a converging–diverging nozzle, also treated by Shuen *et al.* [36]. The parameters are chosen such that regions with very low and medium or high Mach numbers appear. Standard methods for computing incompressible or compressible flow cannot cope with these flows, or at best in an inefficient manner. We use time-stepping starting from rest to converge to steady state, with $\theta = 0.5$ and $\mu = 1$. The following termination criterion is used: $\max_{i,j}((U^{\alpha}_{i,j})^{n+1} - (U^{\alpha}_{i,j})^{n}) \leq \delta t 10^{-6}$.

Two nonstationary test problems were computed as well. The first is the shocktube problem posed by Sod [41], a frequently used test problem for compressible flow solvers. The second is a nonstationary nozzle flow to show that the scheme is suitable for nonstationary weakly compressible flow. For the time stepping method in nonstationary flows the parameters were chosen to be $\theta = 1$ and $\mu = 1$.

4.2. *Stationary Flows*

4.2.1. *Channel with bump. Subsonic flow.* Subsonic flow in a channel with a 10% bump is computed. All equations are discretised using central differences. The size of the channel is $[0, 3] \times [0, 1]$, in which a boundary fitted nonuniform grid of 63×22 cells is generated (see Fig. 2). Results are given for $M_\infty = 0, 10^{-6}, 0.01, 0.1,$ and 0.5. Note that $M_\infty = 0$ is allowed with our method. The boundary conditions are: $\alpha_\infty = 0$, $p_v = 1$. For an inlet Mach number of $M_\infty = 1 \times 10^{-6}$ and 0.5 the resulting iso-Mach lines are shown in Fig. 3. Note that the pattern is symmetric, as it should be for subsonic flow through the specified channel. The computed Mach number distributions on the upper and lower boundary of the channel are compared to results obtained by Eidelman *et al.* [7] in Fig. 3. The results are very similar. Our central scheme gives better symmetry than the (much more computing intensive) second-order upwind-biased Godunov scheme of [7] and contains less numerical diffusion, resulting in a 4% higher maximum Mach number.

Efficiency at low Mach numbers. The number of iterations and CPU time (using a HP9000-735 workstation) required are listed in Table 1. Neither the number of iterations

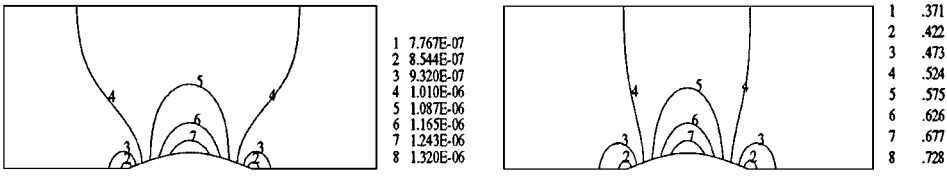

FIG. 3. Mach number contour plot for (a) $M_\infty = 1.10^{-6}$; (b) $M_\infty = 0.5$.

TABLE 1
Channel with 10% Bump, $\delta t = 0.1$

Mach	CPU [s]	Time steps	GMRES iterations	
			Total	Iter/t.step
0.5	151	509	6108	12
0.1	73	220	3960	18
0.01	74	200	4200	21
10^{-6}	74	200	4200	21
0	75	203	4263	21

nor the CPU time deteriorate at low Mach numbers. For increasing Mach numbers the flow takes more time to settle down to steady state, but CPU time per time step does not increase (in fact, it decreases somewhat).

Transonic flow. Although our primary aim is to cover the no-man's land between incompressible and compressible flow, we show in the following examples that the present staggered grid pressure correction method is quite suitable for fully compressible flow as well. In the channel discussed above we take $M_\infty = 0.675$ and obtain transonic flow. In regions of transonic flow the upwind biased approximation for the density as explained in Section 3 is used. Furthermore, for the energy equation a first-order upwind scheme is employed. Again, a boundary-fitted grid of 63×22 cells is used (see Fig. 2). Mach number contours are shown in Fig. 5. The location of the shock was at 70% of the bump, while Eidelman *et al.* [7] found the shock to be at 72%. The maximum Mach number is 1.33 against 1.32 in [7]. At the bump, the shock is captured in four cells.

Supersonic flow. Supersonic flow is computed for a channel with 4% bump and $M_\infty = 1.65$. For this type of flow the first-order upwind scheme is used for the momentum

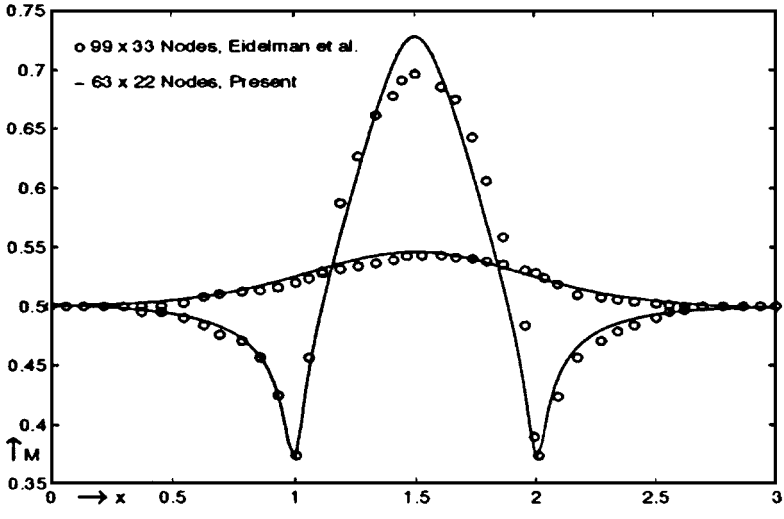

FIG. 4. Mach number at upper and lower boundary of channel with bump for $M_\infty = 0.5$ compared with a second-order Godunov method.

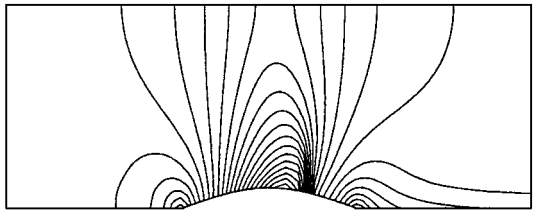

FIG. 5. Mach number contour plot for $M_\infty = 0.675$.

and energy equations. In Fig. 7 the Mach number contours are shown for computation on a 190×55 grid, shown in Fig. 6. The leading edge shock reflects from the top wall and intersects with the shock leaving the trailing edge. All shocks are resolved fairly well, although the reflecting one is somewhat smeared, as is to be expected with a first-order upwind method. In Fig. 8 one can see that the agreement between our first-order accurate results and the results for the second-order Godunov method in [7] (where the grid size is not mentioned) is good; locations of the shocks are the same. Furthermore, it is interesting to note that the shock position does not change with grid refinement (see Fig. 9). The shocks we computed are as sharp as in [7], except for the reflected shock on the upper boundary in the neighbourhood of $x = 2$, and our extreme values are lower than those in [7]. This is most likely due to the use of a first-order upwind scheme for the momentum equations. Compared to the results in [7] for a first-order Godunov method it is found that the present scheme gives better crispness of resolution. A second-order upwind-biased scheme with a limiter can be easily implemented, but our aim here is merely to show the suitability of our scheme for computing supersonic flow.

Viscous flow. Extension to the Navier–Stokes equations is straightforward and will not be described. We give results for the channel with 10% bump with a uniform inlet Mach number of 0.45, just as Shyy in [37]. The grid of 99×49 cells is refined near the wall (see Fig. 10). A laminar computation was performed for a Reynolds number of 4×10^5. The resulting Mach number contours are shown in Fig. 11. These contours are very similar to the results obtained by Shyy [37]. The thickness of the boundary layer is also in agreement. The computing time for low Mach numbers is in the same proportion to the time for $M_\infty = 0.45$ as in the inviscid case.

4.2.2. *Converging–diverging nozzle.* Next, the flow is computed in a converging/diverging nozzle with the following contraction ratios: 5, 10, and 20. The inlet Mach number is kept constant at 0.045. The size of the throat is kept constant at 0.4, and the size of the outlet is kept constant at 2.5 times the size of the throat. For all computations we have used a 49×10

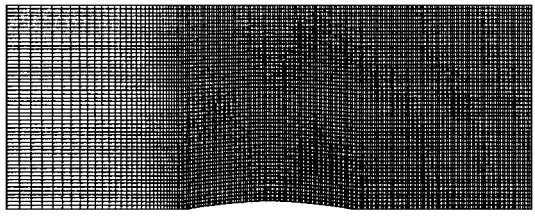

FIG. 6. Grid size 190×55 used for supersonic computations.

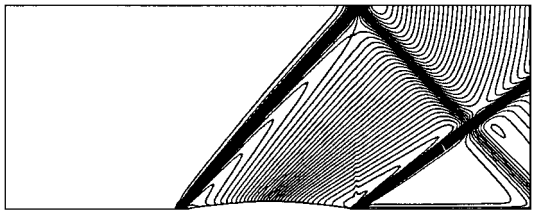

FIG. 7. Mach number contour plot for $M_\infty = 1.65$.

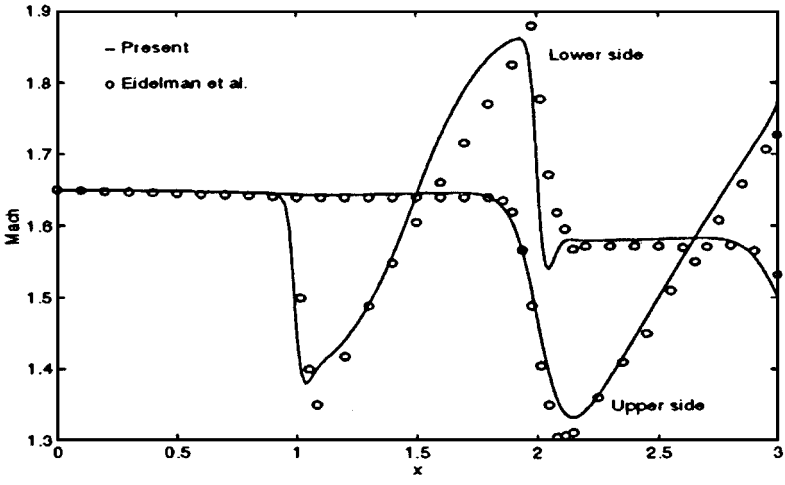

FIG. 8. Mach number at upper and lower boundary of channel with bump for $M_\infty = 1.65$ compared with a second-order Godunov method.

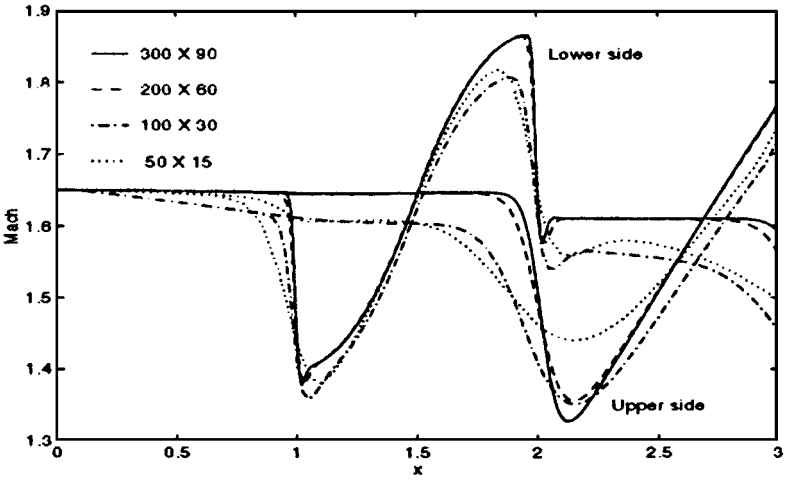

FIG. 9. Mach number at upper and lower boundary of channel with bump with $M_\infty = 1.65$ for different grid sizes.

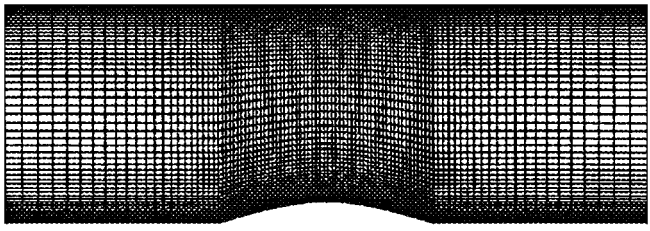

FIG. 10. Grid of size 99×49 used for viscous computation.

nonuniform grid of the type shown in Fig. 12. The time step was kept constant at $\delta t = 0.01$. First-order upwind discretisation was used both in the energy and in the momentum equations. In the computations for flow in nozzles with contraction ratios 5 and 10, the pressure ratio was chosen as $p_v = 1$, and the flow remained subsonic. The maximum Mach numbers that occurred are listed in Table 2. For a contraction ratio of 20, $p_v = 60$ was chosen so that supersonic outflow occurred. In this case a large range of Mach numbers from 0.045 up to 2.34 arose (see Fig. 13). When the solution was computed on a grid with four times as many grid cells, the solution did not change. To obtain convergence on this grid, the time step had to be halved to 0.005.

Efficiency at low Mach numbers. In the nozzle with a contraction ratio of 5 the flow remains virtually incompressible. The maximum Mach number is 0.24. For a contraction ratio of 10 the maximum Mach number is 0.5, for 15 it is 1.82, and for 20 it is 2.67. The CPU time and number of iterations for the nozzle do not increase significantly for lower Mach numbers, that is, smaller contraction ratios. On the contrary, there is an increase of computing time with increasing contraction ratio. This increase of CPU time is caused by the fact that the flow takes longer to settle down to steady state. But the results suffice to illustrate our main point, namely that accuracy and efficiency do not degrade in the presence of low Mach numbers.

4.3. *Nonstationary Flows*

As stated before, one of the advantages of our method over preconditioning methods is that the transient behaviour is not falsified, so that time-accuracy is easily realised. We show results for two nonstationary test cases, namely Sod's shock tube problem test case [41] and a nonstationary flow with low Mach numbers.

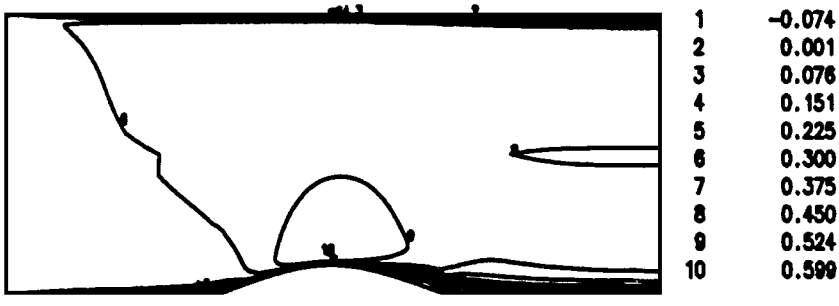

FIG. 11. Mach number contours for $M_\infty = 0.45$ and $\mathrm{Re} = 4 \times 10^5$.

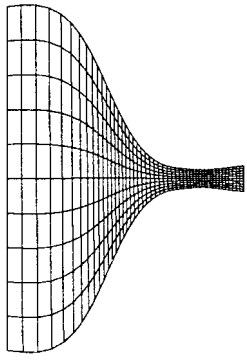

FIG. 12. Grid of size 49×10.

Shock tube problem. Sod's shock tube problem [41] is a Riemann problem with the following left and right states:

$$\rho_1 = p_1 = 1.0, u_1 = 0; \quad \rho_2 = 0.125, p_2 = 0.1, u_2 = 0. \tag{47}$$

Since $w_\infty = 0$ we cannot use the previous nondimensionalisation. Instead we use

$$\rho_r = \rho_1, \quad p_r = p_1, \quad h_r = h_1, \quad w_r = 1. \tag{48}$$

The time discretisation is as before; we take $\Delta x = 0.01$ and $\Delta t = 0.001$. The shock speed is found to be 1.75, corresponding to a Courant number of 0.175. The pressure correction method is used for time-stepping.

For the space discretisation of the momentum and energy equation the first-order upwind scheme was used. Because the flow is subsonic no upwind bias for the density is applied. The difficulties in computing the shock tube problem are to compute the expansion wave and the dicontinuities accurately and to compute the right wave speed. Our solution at $t = 0.15$ is compared with the exact solution at this time in Fig. 14.

Comparison of Fig. 14 with results in [41] shows that our results are as good as those obtained with a first-order Godunov scheme. It shows that our scheme converges to the correct weak solution and satisfies the entropy condition. The contact discontinuity is somewhat smeared due to the use of the first-order upwind scheme. This can be improved by using a higher order upwind scheme. For this we follow the MUSCL approach [46]. Assuming

TABLE 2
Nozzle with Inlet Mach Number of 0.045, δt = 0.01

Contraction ratio	Maximum Mach no.	CPU [s]	Time steps	GMRES iterations	
				Total	Iter/t.step
20	2.67	761	6792	95088	14
15	1.82	750	6790	95060	14
10	.83	220	1866	26124	14
5	.4	300	2744	38416	14

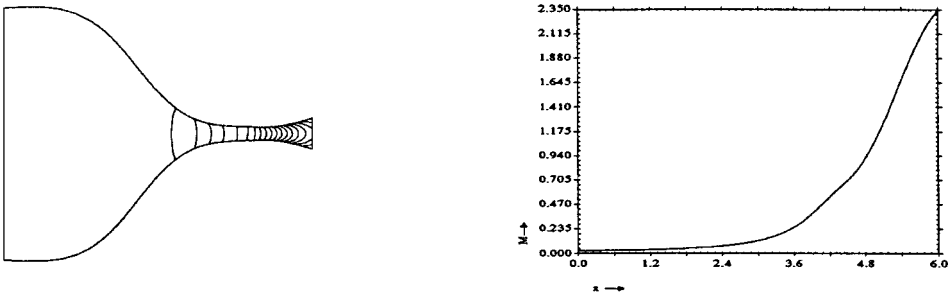

FIG. 13. (a) Mach number contour plot for $M_\infty = 0.045$; (b) Mach number at centerline of nozzle.

$u > 0$, $m_{i+1/2,j}$ is evaluated as

$$m_{i+1/2,j} = m_{i,j} + \frac{1}{2}\Psi(r_{i+1/2})(m_i - m_{i-1}), \tag{49}$$

where

$$r_{i+1/2} = \frac{m_{i+1} - m_i}{m_i - m_{i-1}}, \quad \Psi(r) = \max\left[0, \min\left(2, \frac{1}{2}r + \frac{1}{2}, 2r\right)\right]. \tag{50}$$

The energy equation is handles analogously. In Fig. 15 the solution obtained with the MUSCL scheme is compared to the exact solution. The shock and especially the contact discontinuity have become more crisp. Due to our nonconservative discretisation of the energy equation, a tiny wiggle is formed in front of the contact discontinuity. The staggered scheme seems to be as accurate as nonstaggered schemes based on approximate Riemann solvers and flux limiting (see, for example, similar results [1, 13, 14].

Nonstationary nozzle. In order to test the method on a nonstationary low Mach number flow, we have computed flow in the converging/diverging nozzle of Section 4.2.2 with nonstationary inflow. In this case the inlet Mach number M_∞ varied between 0 and 0.045 with a period of 0.5 s. The resulting Mach number at the center line is plotted in Fig. 16. No particular difficulties were encoutered.

5. CONCLUDING REMARKS

A method to compute flows has been described that has accuracy and efficiency uniform for very low and medium Mach numbers. A nondimensionalisation has been introduced

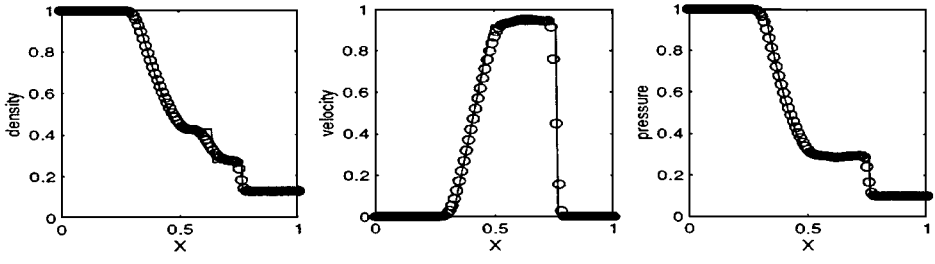

FIG. 14. Comparison of first-order upwind scheme with exact solution.

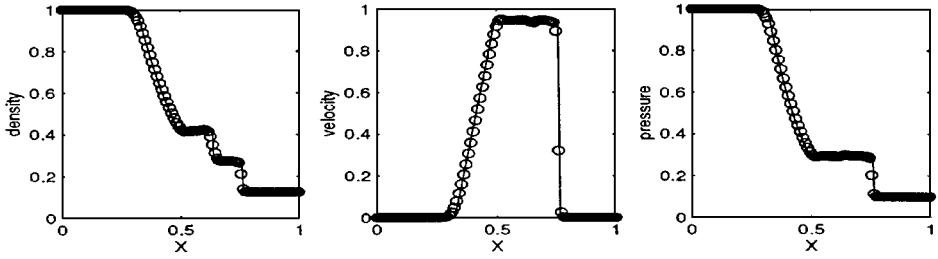

FIG. 15. Comparison of MUSCL scheme with exact solution.

such that all quantities in the dimensionless Euler equations remain finite and $\mathcal{O}(1)$ when the Mach number goes to zero. The dimensionless equations are discretised in general coordinates on a staggered grid and solved with a pressure correction method and implicit time stepping. From the numerical experiments the following conclusions can be drawn:

- Good results are obtained for low Mach number flow, including $M = 0$.
- Mach number independent convergence is observed for subsonic flow.
- The staggered scheme is also accurate for fully compressible, transonic, and supersonic flow. The Rankine–Hugoniot and entropy conditions seem to be satisfied.
- Time discretisation is straightforward. Nonstationary flows can be efficiently and accurately computed for Mach numbers ranging from zero to supersonic.

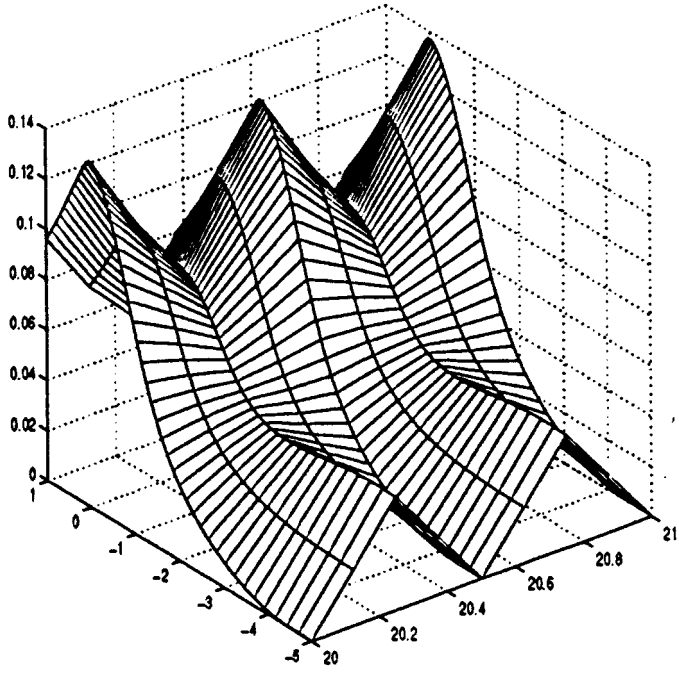

FIG. 16. Nonstationary nozzle.

REFERENCES

1. M. Arora and P. L. Roe, A well-behaved TVD limiter for high-resolution calculations of unsteady flow, *J. Comput. Phys.* **132**, 3 (1997).
2. W. R. Briley, H. McDonald, and S. J. Shamroth, A low Mach number Euler formulation and application to time-iterative LBI schemes, *AIAA J.* **21**, 1467 (1983).
3. D. R. Chenoweth and S. Paolucci, Natural convection in an enclosed vertical air layer with large horizontal temperature differences, *J. Fluid Mech.* **169**, 173 (1986).
4. Y.-H. Choi and C. L. Merkle, The application of preconditioning in viscous flows, *J. Comput. Phys.* **105**, 207 (1993).
5. L. Davidson and P. Hedberg, Mathematical derivation of a finite volume formulation for laminar flow in complex geometries, *Int. J. Num. Meth. Fluids*. **9**, 531 (1989).
6. I. Demirdžić, Z. Lilek, and M. Perić, A collocated finite volume method for predicting flows at all speeds, *Int. J. Num. Meth. Fluids* **16**, 1029 (1993).
7. S. Eidelman, P. Colella, and R. P. Shreeve, Application of the Godunov method and its second-order extension to cascade flow modelling, *AIAA J.* **22**, 1609 (1984).
8. A. G. Godfrey, R. W. Walters, and B. van Leer, Preconditioning for the Navier–Stokes equations with finite rate chemistry, AIAA Paper 93-0535, 1993.
9. J. Guerra and B. Gustafsson, A numerical method for incompressible and compressible flow problems with smooth solutions, *J. Comput. Phys.* **63**, 377 (1986).
10. F. H. Harlow and A. A. Amsden, Numerical calculation of almost incompressible flows, *J. Comput. Phys.* **3**, 80 (1968).
11. F. H. Harlow and A. A. Amsden, A numerical fluid dynamics calculation method for all flow speeds, *J. Comput. Phys.* **8**, 197 (1971).
12. F. H. Harlow and J. E. Welch, Numerical calculation of time-dependent viscous incompressible flow of fluid with a free surface, *The Physics of Fluids* **8**, 2182 (1965).
13. A. Harten, High resolution schemes for hyperbolic conservation laws, *J. Comput. Phys.* **49**, 357 (1983).
14. A. Harten, B. Engquist, S. Osher, and S. R. Chakravarty, Uniformly high order accurate essentially non-oscillatory schemes, III, *J. Comput. Phys.* **71**, 231 (1987).
15. A. Hosangadi, C. L. Merkle, and S. R. Turns, Analysis of forced combusting jets, *AIAA J.* **28**, 1473 (1990).
16. T. Ikohagi, B. R. Shin, and H. Daiguji, Application of an implicit time-marching scheme to a three-dimensional incompressible flow problem in curvilinear coordinate systems, *Computers and Fluids* **21**, 163 (1992).
17. R. I. Issa, A. D. Gosman, and A. P. Watkins, The computation of compressible and incompressible flows by a non-iterative implicit scheme, *J. Comput. Phys.* **62**, 66 (1986).
18. R. I. Issa, Solution of the implicitly discretised fluid flow equations by operator-splitting, *J. Comput. Phys.* **62**, 40 (1986).
19. S. M. H. Karimian and G. E. Schneider, Pressure-based control volume finite element method for flow at all speeds, *AIAA J.* **33**, 1611 (1995).
20. K. C. Karki and S. V. Patankar, Pressure based calculation procedure for viscous flows at all speed in arbitrary configurations, *AIAA J.* **27**, 1167 (1989).
21. S. Klainerman and A. Majda, Singular limits of quasilinear hyperbolic systems with large parameters and the incompressible limit of compressible fluids, *Comm. Pure Appl. Math.* **34**, 481 (1981).
22. S. Klainerman and A. Majda, Compressible and incompressible flows, *Comm. Pure Appl. Math.* **35**, 629 (1982).
23. R. Klein, Semi-implicit extension of a godunov-type scheme based on low mach number asymptotics 1: One-dimensional flow, *J. Comput. Phys.* **121**, 213 (1995).
24. S. Koshizuka, Y. Oka, and S. Kondo, A staggered differencing technique on boundary-fitted curvilinear grids for incompressible flows along curvilinear or slant walls, *Computational Mechanics* **7**, 123 (1990).

25. H. O. Kreiss, J. Lorenz, and M. J. Naughton, Convergence of the solutions of the compressible to the solutions of the incompressible Navier–Stokes equations, *Adv. Appl. Math.* **12**, 187 (1991).
26. A. Majda, *Compressible Fluid Flow and Systems of Conservation Laws in Several Space Variables*, *Applied Mathematical Sciences*, Vol. 53 (Springer-Verlag, New York, 1984).
27. P. A. McMurtry, W. H. Jou, J. J. Riley, and R. W. Metcalfe, Direct numerical simulations of a reacting mixing layer with chemical heat release, *AIAA J.* **24**, 962 (1986).
28. C. L. Merkle and Y.-H. Choi, Computation of low-speed compressible flows with time marching procedures, *Int. J. Numer. Methods Eng.* **25**, 831 (1988).
29. K. Morinishi, Comparison of numerical solutions of pseudocompressible flows and compressible flows at low Mach numbers, AIAA Paper 92-2648, 1992.
30. E. S. Oran and J. P. Boris, Detailed modelling of combustion systems, *Prog. Energy Combust. Sci.* **7**, 1 (1981).
31. R. L. Panton, *Incompressible Flow* (Wiley, New York, 1984).
32. G. Patnaik, R. H. Guirguis, J. P. Boris, and E. S. Oran, A barely implicit correction for flux-corrected transport, *J. Comput. Phys.* **71**, 1 (1987).
33. R. G. Rehm and H. R. Baum, The equations of motion for thermally driven buoyant flows, *J. Res. Nat. Bur. Stand.* **83**, 297 (1978).
34. M. Rosenfeld, D. Kwak, and M. Vinokur, A fractional step solution method for the unsteady incompressible Navier–Stokes equations in generalized coordinate systems, *J. Comput. Phys.* **94**, 102 (1991).
35. A. Segal, P. Wesseling, J. van Kan, C. W. Oosterlee, and K. Kassels, Invariant discretization of the incompressible Navier–Stokes equations in boundary fitted co-ordinates, *Int. J. Num. Meth. Fluids* **15**, 411 (1992).
36. J.-S. Shuen, K.-H. Chen, and Y. Choi, A coupled implicit method for chemical non-equilibrium flows at all speeds, *J. Comput. Phys.* **106**, 306 (1993).
37. W. Shyy, A numerical study of two-dimensional compressible Navier–Stokes flows, *Num. Heat Transfer* **14**, 323 (1988).
38. W. Shyy and M. E. Braaten, Adaptive grid computation for inviscid compressible flows using a pressure correction method, AIAA Paper 88-3566-CP, 1988.
39. W. Shyy, M.-H. Chen, and C.-S. Sun, Pressure-based multigrid algorithm for flow at all speeds, *AIAA J.* **30**, 2660 (1992).
40. W. Shyy, S. S. Tong, and S. M. Correa, Numerical recirculating flow calculation using a body fitted coordinate system, *Numerical Heat Transfer* **8**, 99 (1985).
41. G. A. Sod, A survey of several finite difference methods for systems of nonlinear conservation laws, *J. Comput. Phys.* **27**, 1 (1978).
42. M. C. Thompson and J. H. Ferziger, An adaptive multigrid technique for the incompressible Navier–Stokes equations, *J. Comput. Phys.* **82**, 94 (1989).
43. E. Turkel, Review of preconditioning techniques for fluid dynamics, *Appl. Num. Math.* **12**, 257 (1993).
44. E. Turkel, A. Fiterman, and B. van Leer, Preconditioning and the limit to the incompressible flow equations, Report 93-42, ICASE, NASA Langley, 1993.
45. J. J. I. M. Van Kan, A second-order accurate pressure correction method for viscous incompressible flow, *SIAM J. Sci. Stat. Comput.* **7**, 870 (1986).
46. B. van Leer, Towards the ultimate conservative difference scheme. V. A second-order sequel to Godunov's method, *J. Comput. Phys.* **32**, 101 (1979).
47. B. van Leer, W.-T. Lee, and P. L. Roe, Characteristic time-stepping or local preconditioning of the Euler equations, AIAA Paper 91-1552, 1991.
48. S. Venkateswaran, C. L. Merkle, and S. T. Thynell, Analysis of direct solar thermal rocket propulsion, *J. Propulsion Power* **8**, 541 (1992).
49. H. Viviand, Pseudo-unsteady systems for steady inviscid flow calculations, in *Numerical Methods for the Euler Equations of Fluid Dynamics* (F. Angrand, A. Dervieux, and J. A. Désidéri, Eds.) (SIAM, Philadelphia, 1985), p. 334.

50. C. Vuik, Fast iterative solvers for the discretized incompressible Navier–Stokes equations, *Int. J. Num. Meth. Fluids* **22**, 195 (1996).
51. J. P. Withington, J. S. Shuen, and V. Yang, A time accurate implicit method for chemically reacting flows at all Mach numbers, AIAA Paper 91-0581, 1991.
52. M. Zijlema, A. Segal, and P. Wesseling, Finite volume computation of incompressible turbulent flows in general coordinates on staggered grids, *Int. J. Num. Meth. Fluids* **20**, 621 (1995).
53. M. Zijlema, A. Segal, and P. Wesseling, Invariant discretization of the k-ε model in general co-ordinates for prediction of turbulent flow in complicated geometries, *Computers and Fluids* **24**, 209 (1995).